



## OPEN ACCESS

## EDITED BY

Weiqiang Chen,  
Rice University, United States

## REVIEWED BY

Zhongnian Yang,  
Qingdao University of Technology, China  
Yuanchao Zhang,  
Fuzhou University, China

## \*CORRESPONDENCE

Jie Xu,  
✉ ts20030211p31@cumt.edu.cn  
Wen-Ling Tian,  
✉ tb21220018b2@cumt.edu.cn

RECEIVED 08 March 2024

ACCEPTED 28 March 2024

PUBLISHED 16 April 2024

## CITATION

Xu J, Tian W-L, Bu Y-S and Yang J (2024),  
Experimental study on mechanical properties  
and microscopic mechanisms of layered  
sandstone after high temperature water  
cooling.  
*Front. Earth Sci.* 12:1394855.  
doi: 10.3389/feart.2024.1394855

## COPYRIGHT

© 2024 Xu, Tian, Bu and Yang. This is an  
open-access article distributed under the  
terms of the [Creative Commons Attribution  
License \(CC BY\)](https://creativecommons.org/licenses/by/4.0/). The use, distribution or  
reproduction in other forums is permitted,  
provided the original author(s) and the  
copyright owner(s) are credited and that the  
original publication in this journal is cited, in  
accordance with accepted academic practice.  
No use, distribution or reproduction is  
permitted which does not comply with  
these terms.

# Experimental study on mechanical properties and microscopic mechanisms of layered sandstone after high temperature water cooling

Jie Xu<sup>1\*</sup>, Wen-Ling Tian<sup>1\*</sup>, Yi-Shun Bu<sup>2</sup> and Jing Yang<sup>3</sup>

<sup>1</sup>School of Mechanics and Civil Engineering, China University of Mining and Technology, Xuzhou, Jiangsu, China, <sup>2</sup>School of Civil Engineering and Architecture, Anhui University of Science and Technology, Huainan, Anhui, China, <sup>3</sup>State Key Laboratory of Mining Response and Disaster Prevention and Control in Deep Coal Mines, Anhui University of Science and Technology, Huainan, Anhui, China

During underground resource extraction and deep underground engineering development, the engineering rock body frequently encounters elevated temperatures and water cooling, leading to alterations in the mechanical properties of the rock. These changes will have an impact on the safety and stability of the project. This study aimed to investigate the changes in mechanical properties of rocks following treatment with high temperatures and water cooling. The experiment involved subjecting layered sandstone samples to heating and water cooling, followed by conducting uniaxial compression tests using a high-temperature furnace and a WA-1000 universal testing machine. The effects of temperature and inclination angles on the uniaxial mechanical properties of layered sandstone were then analyzed. Furthermore, the utilization of the scanning electron microscope and various other microscopic testing devices allowed for the examination of the micro-mechanism behind rock damage and rupture subsequent to undergoing heating and water-cooling treatment. The findings from the experiment suggest that: 1) the relationship between the changes in sandstones' mechanical properties and temperature and bedding inclinations can be attributed to the uneven deformation of minerals caused by heating and water-cooling treatment, leading to the distribution of microcracks within the rock. 2) The stress-strain curve of the specimen can be divided as four-stages. With the increase of bedding inclination, the compaction stage of the specimen is more prominent. 3) As the bedding inclination increases, the specimens exhibit a pattern of initially decreasing and then increasing in terms of peak strength and strain. With the increase of temperature, the peak axial strain gradually increases, while it first increases and then decreases with the increasing dip angles.

## KEYWORDS

rock mechanics, high temperature treatment, water cooling, bedding angle, deformation characteristics

## 1 Introduction

Underground resource extraction and underground engineering construction are often accompanied by high temperature (Sirdesai et al., 2017a; Huang et al., 2017; Zhu et al.,

2018), and the mechanical properties of rocks undergoing high temperatures show different states with the variation of temperature (Liu and Xu, 2014; Gautam et al., 2016; Su et al., 2016; Sirdesai et al., 2017b). For some practical projects (e.g., coal mine fires, dry hot rocks, etc.), rocks exposed to high temperatures often experience quick cooling when submerged in water, and the mechanical characteristics of rocks following rapid cooling significantly impact the security of subterranean projects (Kang et al., 2021).

Sandstone, being a typical type of sedimentary rock, displays a distinct arrangement of layers. As the weak factor, the bedding surface often determines the strength and stability of sandstone (Zhou et al., 2019). The mechanical properties and damage modes are also significantly affected by the bedding angle and the stress level (Hu et al., 2017). The peak strength of different layered rocks is highly subjective to the layer angle, which is determined by various parameters including mineral composition, mineral size, pore distribution, and spacing of the bedding in different layered rocks. Based on experimental studies, it has been observed that the maximum peak stress in bedding sandstones occurs at an angle of 0°, while the minimum peak stress varies depending on the structural anisotropy of the bedding rocks (Rawling et al., 2002; Zhang et al., 2010). This minimum peak stress angle is approximately within the range of 30°–67.5°, which also coincides with the point of the rock body's smallest energy storage limit (Donath, 1972; Dunn et al., 1973; Yan et al., 2023). The anisotropy of the longitudinal wave velocity and elastic modulus is also observed. The longitudinal wave velocity gradually increases as the layered inclination angle increases, while the change in elastic modulus with bedding direction is similar with that of strength, exhibiting a “U-shaped” variation (Yin and Yang, 2018; Shi et al., 2020). Three different failure mechanisms are observed when the specimen is damaged: 1) splitting damage throughout the specimen; 2) sliding damage along the laminar surface; and 3) a mixture damage of splitting and sliding (Yang et al., 1998). Laminated rocks with small angular inclinations have more drastic damage patterns than those with large angular inclinations (Wasantha et al., 2014).

Mechanical properties and micro-mechanisms of thermal damage in rocks can be studied with the help of micro-testing methods (SEM, X-ray diffraction and CT scanning, etc.) (Zhao et al., 2018; Zhou et al., 2020). The temperature range of 400°C–600°C was discovered to be the critical interval that impacts the alteration of sandstone's physical and mechanical characteristics following exposure to high temperatures (Guo et al., 2017; Zhang et al., 2019; Dong et al., 2020). According to, the temperature prior to the critical temperature can be categorized into three phases depending on the release temperature of attached water, boundary water, and structural water within the rock (Zhang et al., 2016). The rise in temperature causes water to be released and particles to expand, leading to the gradual filling of the initial pores and cracks. This process ultimately strengthens the mechanical characteristics of the sandstone (Ranjith et al., 2012; Gautam et al., 2018). As the temperature rises above the critical point, the particles undergo continuous expansion, resulting in the formation of fresh pores and cracks. This, in turn, causes a decline in the sandstones' physical attributes (including mass, density, dynamic peak strength, elastic modulus, P-wave and S-wave velocities) (Sun et al., 2016; Yang et al., 2017; Yang et al., 2023), as well as their mechanical properties (such as uniaxial and triaxial compressive strengths,

elastic modulus) (Ding et al., 2016). After undergoing various cooling techniques like natural cooling (Zhao et al., 2023), water cooling, and liquid nitrogen cooling (Zhang et al., 2020), high-temperature rocks exhibit notable variations in their mechanical characteristics and modes of failure. The specimen experiences thermal shock when it is rapidly cooled in water, leading to an increase in cracks due to the non-directional heat transfer caused by the thermal shock. Hydraulic action also fluidizes rock particles, leading to an increase in rock porosity and permeability (Ma et al., 2022a; Ma et al., 2022b; Ma et al., 2022c). Over time, the fissures slowly intersect and infiltrate, creating a network of tiny cracks that negatively impact the mechanical characteristics. The values of the uniaxial compressive strength, elastic modulus, and tensile strength are all less than those of the specimen following natural cooling (Wu et al., 2021; Yang et al., 2021; Zhu et al., 2021; Chen et al., 2022). In addition, when water cools rapidly, it also heightens the thermal resistance between mineral particles, diminishes thermal conductivity, intensifies the concentration of stress in specific areas, and augments the disparity in local bearing capacity. Consequently, all of these factors contribute to the improvement of the rock samples' ductile characteristics (Nin et al., 2021). On the other hand, the use of liquid nitrogen immersion cooling method creates a distinct difference in temperature, causing the microporous structure within the high-temperature rock samples to expand. This expansion leads to the clustering of microcracks, resulting in wider cracks, improved connectivity of crack networks, and a higher concentration of cracks. Consequently, this leads to a significant deterioration of the mechanical properties (Wu et al., 2019; Yang et al., 2019; Cai et al., 2022).

Extensive research has been conducted on the mechanical attributes of layered stone and the properties of stone following various cooling techniques. However, there has been limited investigation into the mechanical properties of layered sandstone, a prevalent rock formation in deep engineering, subsequent to undergoing thermal treatment. In order to further analyze the mechanical properties of bedded sandstone after high temperature and water-cooling treatment, and explore the microscopic mechanism of high temperature, this study focuses on layered sandstone and utilizes XRD, SEM, and uniaxial compression test to examine the mechanical characteristics of sandstone following treatment with high temperatures and water-cooling. Additionally, it explores the impact of temperature and inclination angle on the mechanical properties of sandstone. The findings aim to offer insights for assessing the stability of rock projects, like tunnels, after being subjected to high-temperature water-cooling, such as extinguishing fires with water.

## 2 Test materials and methodologies

### 2.1 Characterization and preparation of rock samples

The rock specimens used in the test were sampled from Rizhao, Shandong Province, China, and appeared to be layered red sandstone, the average density of the rock samples is 2.23 g/cm<sup>3</sup> in

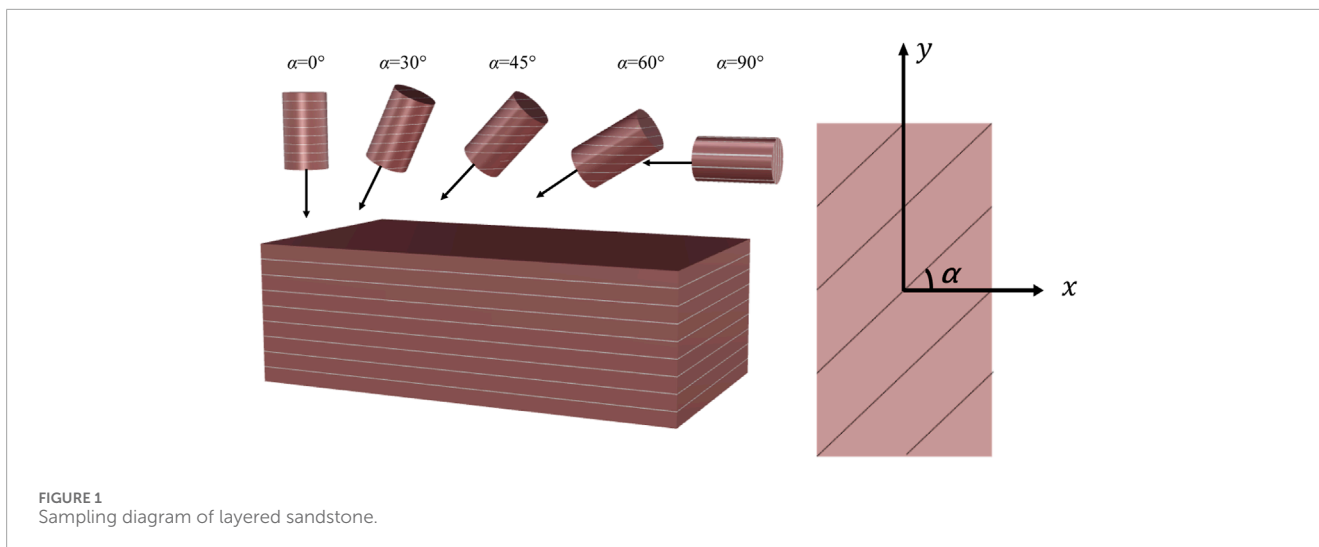


FIGURE 1 Sampling diagram of layered sandstone.

the natural state, and the porosity is 14% as measured by the water-saturated method. To maintain the uniformity of the specimens, all the samples utilized in this study were extracted from the identical block through drilling. The angle between the stratigraphic plane and the horizontal plane was defined as the bedding inclination  $\alpha$ . The bedding angle of the rock mass was always kept horizontal during coring, and by adjusting the tilt angle of the drill bit, a total of five groups of sandstone samples with different bedding angles of 0°, 30°, 45°, 60° and 90° were obtained, and the schematic diagram of the samples is shown in Figure 1, which was made into a standard specimen of 100 mm in height, 50 mm in diameter, and the height-to-diameter ratio is 2, which is in line with the standard of the International Society for Rock Mechanics (ISRM).

The processed specimens are put into the box-type electric resistance furnace (SX2-12-12A) for heating treatment, and the preset temperatures are 300°C, 450°C, 600°C, and 750°C, respectively, and only one sample was prepared for each cooling group. After heated to the preset temperature at a heating rate of 5°C/min, the sample was kept in the furnace for 2 h to ensure uniform heating. After the heat preservation, the sample was directly put into the water bath for rapid cooling with a cooling temperature at 25°C ± 0.5°C for 2 h to ensure that the sample is completely cooled. The sample number is in the form of RA-B, where R represents layered red sandstone; A represents the bedding angle; B represents the heating temperature (the values 1, 2, 3, 4, and 5 indicate 25°C, 300°C, 450°C, 600°C, and 750°C, respectively).

Figure 2 demonstrates the XRD results of red sandstone heating and water-cooling treatment at various temperatures. As seen in Figure 2, the mineral composition of the rock specimen in the natural state is mainly quartz crystals, calcium compounds, sodium feldspar and iron oxides. At temperatures of 300°C and 450°C, there was no significant alteration in the internal mineral composition of the samples. While the internal composition of the specimen showed a significant change for quartz crystals, sodium feldspar, and potassium feldspar when the temperature reached 600°C. When the temperature was further increased to 750°C, the sample mineral composed of quartz crystals, sodium feldspar, and calcium oxide. In summary, the quartz and sodium feldspar compositions did not

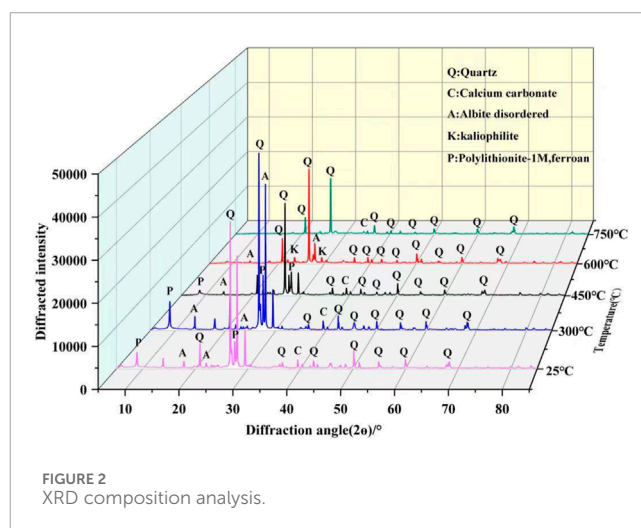


FIGURE 2 XRD composition analysis.

change at high temperatures, but the calcium compounds and iron compounds in the specimen changed as the temperature increased.

## 2.2 Testing equipment

In Figure 3A, the box-type resistance furnace SX2-12-12A is displayed, which is utilized for heating the specimen and has the capability to achieve a maximum heating temperature of 1,200°C. The WAW-1000 universal testing machine (depicted in Figure 3) was utilized to conduct the uniaxial loading test. The maximum axial load of Figure 3B is 1,000 kN, with a loading rate range of 0.1–100 mm/min and an accuracy class of 0.5.

## 2.3 Experimental scheme

The sample was raised to the target temperature (25°C, 300°C, 450°C, 600°C, and 750°C) at a heating rate of 10°C/min, kept

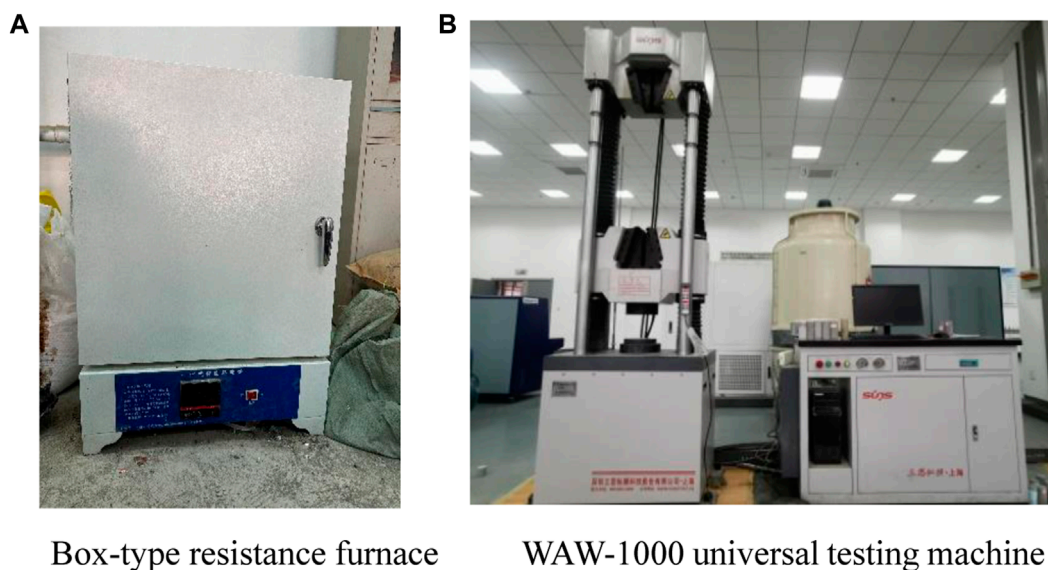


FIGURE 3 Test apparatus. (A) Box-type resistance furnace. (B) WAW-1000 universal testing machine

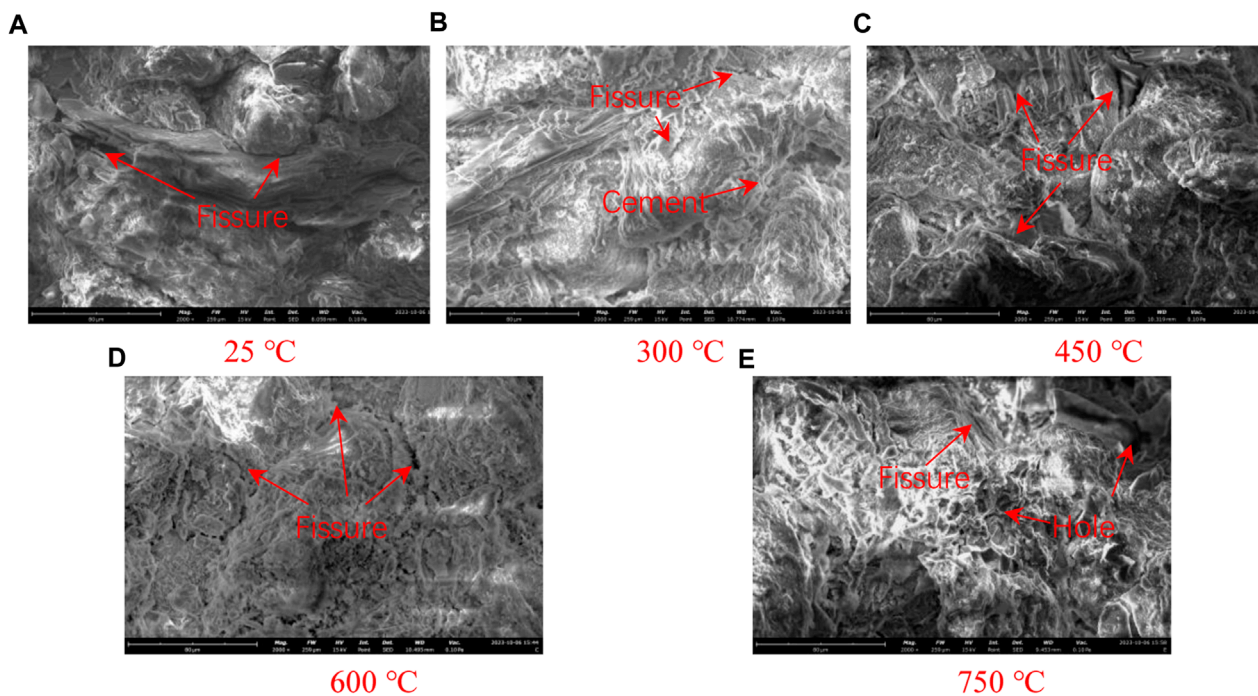


FIGURE 4 SEM microstructure of layered sandstone after high temperature. (A) 25°C. (B) 300°C. (C) 450°C. (D) 600°C. (E) 750°C.

constant for 2 h, and then put into water to cool to room temperature, and there are five cases of bedded inclination angle  $\alpha$  of 0°, 30°, 45°, 60° and 90° in each temperature group. After conducting XRD and SEM micro-tests on the thermally treated specimens, uniaxial compression tests were performed at a loading rate of 0.1 mm/min.

### 3 Experimental results

#### 3.1 Microscopic properties

The variation in the macroscopic mechanical property of rocks after high temperatures is a reflection of the variation in the

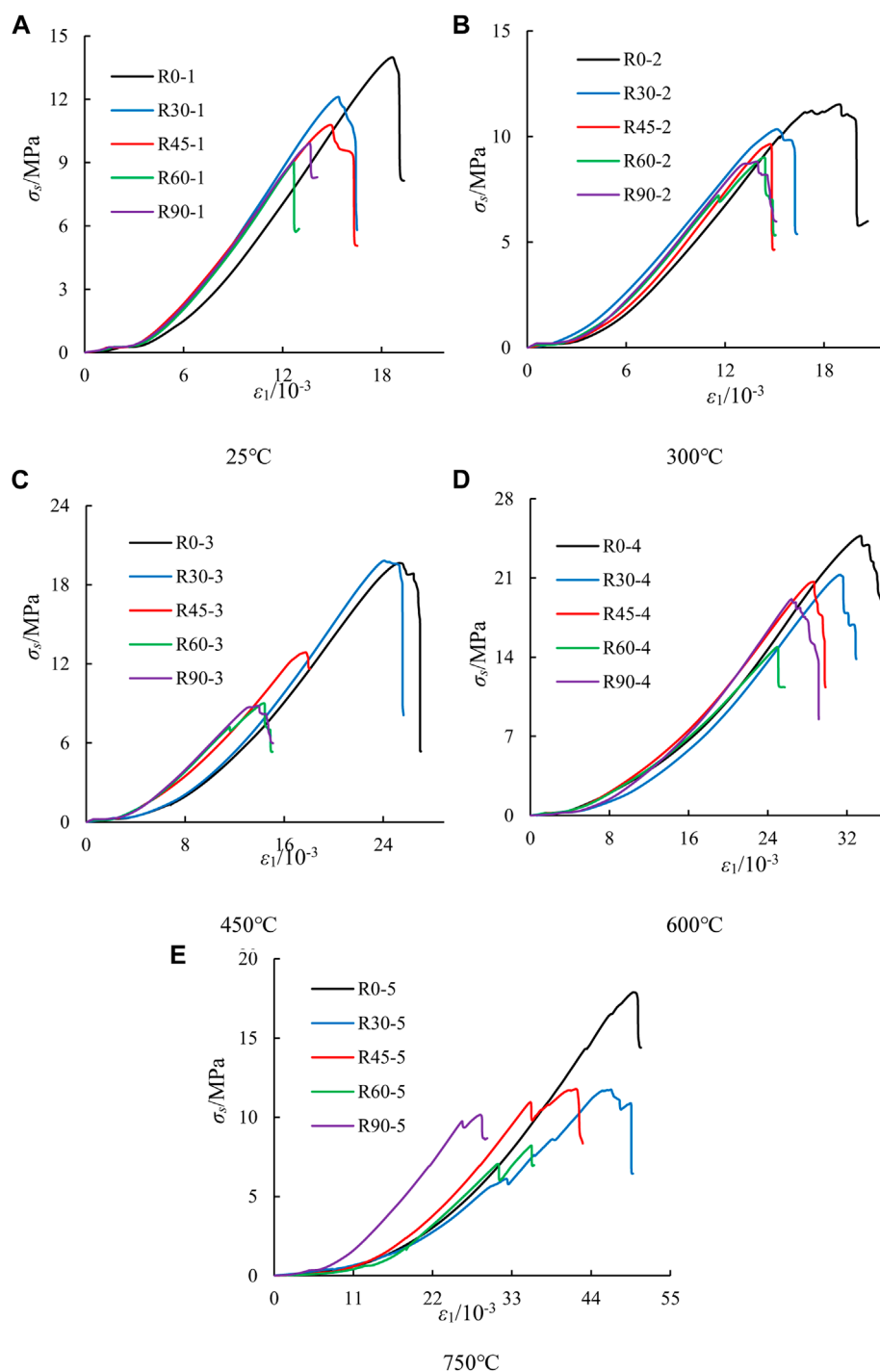


**FIGURE 5** Axial stress-strain curves for the layered sandstone specimens with varying inclination angles after the same heat treatment. (A) 25°C. (B) 300°C. (C) 450°C. (D) 600°C. (E) 750°C.

internal micro-structure (Fan et al., 2020). The rock undergoes irregular deformation at high temperatures due to variations in the expansion coefficients of its mineral grains, leading to the formation of thermal cracks and subsequent alteration of its mechanical characteristics. Figure 4 displays the microscopic alterations of the

rock at various temperatures to demonstrate the progression of mechanical characteristics in the layered sandstone under elevated temperatures.

Figure 4A depicts the microstructure of layered sandstone at room temperature, with good ordering between the mineral

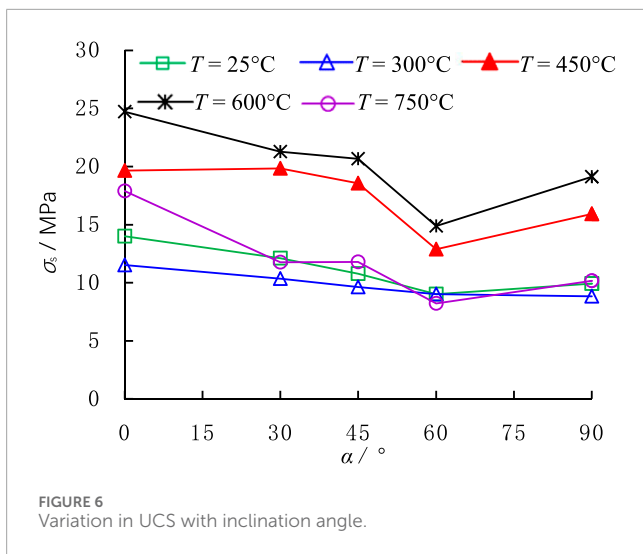


FIGURE 6 Variation in UCS with inclination angle.

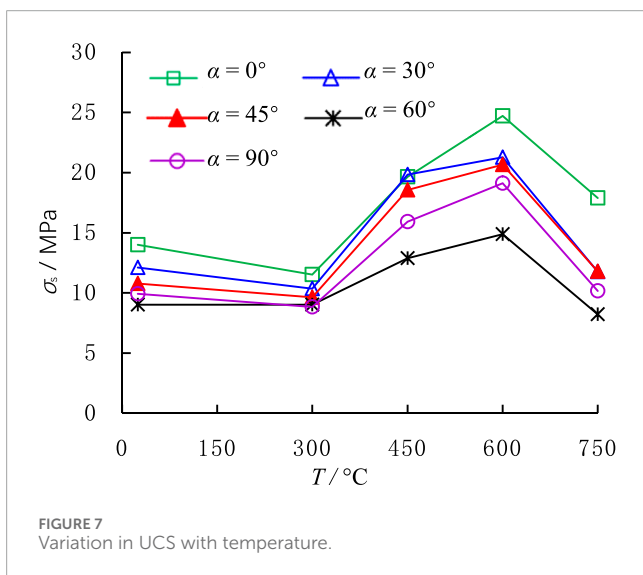


FIGURE 7 Variation in UCS with temperature.

particles of the original specimen, and a small number of micro-cracks were observed between some mineral particles. As the temperature increases, the inhomogeneous expansion of the minerals causes thermal cracks to initiate between the grains. Under the action of water cooling, the plastic deformation produced by the internal particles of the rock could not be recovered, thus causing the phenomenon that the thermal-induced cracks gradually increase with the increasing temperature, as shown in Figures 4B, C. As the temperature rises above 600°C, the internal cementation of the specimen gradually increases. Under the action of high temperature, some of the cemented material will be dissolved and then re-coalesced into new substances after water cooling. As shown in Figure 4D, as the temperature reaches 600°C, the rock exhibits a greater presence of visible micro-cracks and micro-pores, with a more

intricate network of intersecting micro-cracks. The water-cooling effect caused the rock particles to produce unrecoverable plastic deformation, making the internal particle cementation state worse. At a temperature of 750°C, the disarray of the grains and fractures in the rock intensifies. Further due to the increase of cracks between the particles, a series of changes in composition occur, and deposition occurs when the composition is cooled by water.

### 3.2 Stress-strain curve

The uniaxial stress-strain curves of layered sandstone with different inclination angles at different temperatures are presented in Figure 5. The stress-strain curves of various specimens can be categorized into four stages: fracture compaction stage, elastic deformation stage, inelastic deformation stage, and destruction stage, which are observable. During the natural process of rock formation, gaps and cavities will develop between various particles in the rock. These gaps will gradually shrink and close as the rock is subjected to stress during the initial loading phase. The relationship between stress and strain at this stage is nonlinear, which is called the fracture compaction stage. Upon compaction of the fissures among the particles, the loading process exhibited a direct relationship between stress and strain, resulting in an almost linear stress-strain curve. This phase is commonly referred to as the stage of elastic deformation. With the gradual accumulation of internal damage, the stress-strain curve of the specimen transits from the elastic phase to the nonlinear phase until the specimen strength reaches the peak (the maximum limit of the rock specimen that can be loaded), which corresponds to the inelastic deformation phase. Upon reaching the point of maximum load-bearing capacity, a significant quantity of fractures within the rock persistently propagation, resulting in the formation of visible cracks. The specimen's bearing capacity decreases quickly after damage due to the absence of circumferential pressure limitation, as evidenced by the rapid decline in post-peak stress, indicating typical brittle damage characteristics.

To further examine the impact of varying bedding angles on the mechanical and deformation properties of the samples, a comparison was made between the stress-strain curves of the sandstone with different temperatures, as depicted in Figure 5. Figure 5 reveals variations in stress-strain curves among specimens with varying bedding angles at identical temperatures, with the most significant disparity occurring following exposure to 750°C. The compaction phase of the sample is most apparent and the maximum strength of the sample is also the highest at  $\alpha = 0^\circ$ , while the compaction phase and peak strength seemed to be diminished at other inclinations. The stress-strain curve of the specimen becomes less steep as the bedding angle increases, and the compaction stage becomes more pronounced, suggesting that the bedding angle has an impact on the stress-strain curve of the specimen. The results of the study indicate that in actual projects, it is more helpful to ensure the safety of the project if mining is carried out along the horizontal direction of the strata.

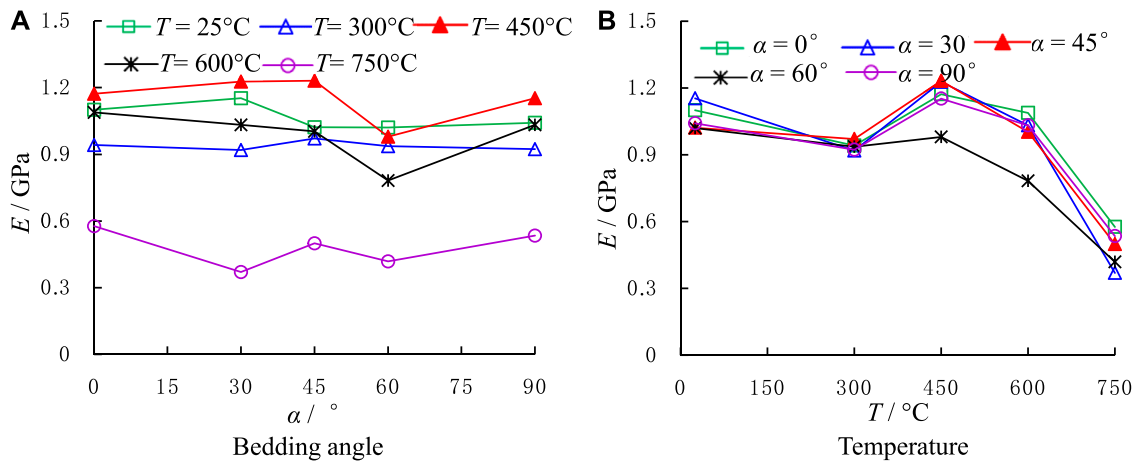


FIGURE 8 Variation of elastic modulus with bedding inclination and temperature. (A) Bedding angle. (B) Temperature.

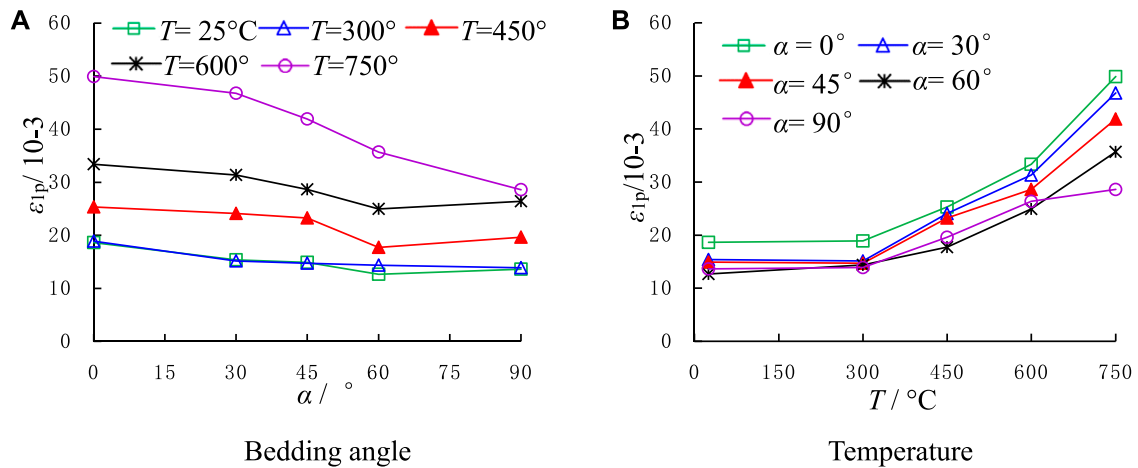


FIGURE 9 Variation of peak strain with bedding inclination and temperature. (A) Bedding angle. (B) Temperature.

### 3.3 Strength characteristics of layered sandstone

Figure 6 illustrates the correlation between the inclination of bedding and the maximum resistance of samples at identical temperatures. Peak strength of layered sandstone shows a “V” type trend with increasing bedding angle, which decreases first and increases later. The lowest strength is found at  $\alpha = 60^\circ$ , and the highest strength is found at  $\alpha = 0^\circ$ . If the specimen is damaged by sliding along the surface of the laminate, which is the weak surface of the rock structure, its bearing capacity will be greatly reduced, which often occurs in the specimen when  $\alpha = 60^\circ$ . This phenomenon shows that in practical engineering, the specimen is most likely to be damaged when the stratum is located in the rock when  $\alpha = 60^\circ$ .

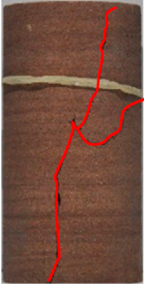
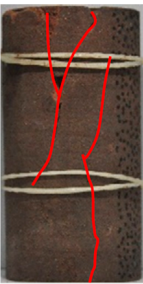
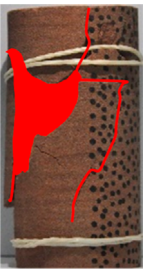
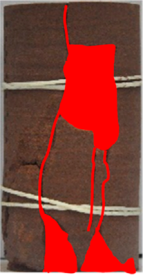
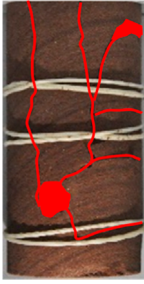
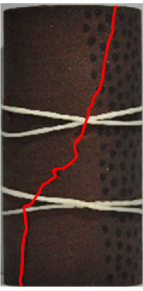
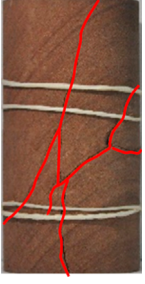
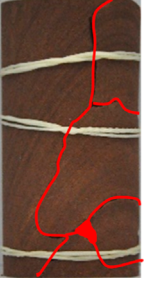
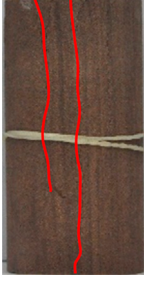
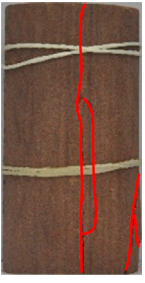
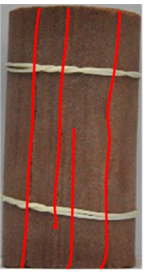
Figure 7 presents the relationship between temperature and the peak strength at the same bedding angle. The specimen’s overall peak strength exhibits a trend of decreasing, then rising, and

then decreasing again as the temperature increases. The specimen’s strength is slightly lower at 300°C compared to room temperature, but it gradually rises as the temperature reaches 600°C before declining again at 750°C. The sandstone’s durability increased from 300°C to 600°C, but declined beyond 600°C. After water cooling at 900°C, the specimens cracked along the stratum, and the grains were broken up and dispersed in the water in the form of sediment. In brief, the impact of subjecting sandstone to high temperatures and water cooling aligns with the identical trend observed for a specific bedding angle.

### 3.4 Deformation characteristics of layered sandstone

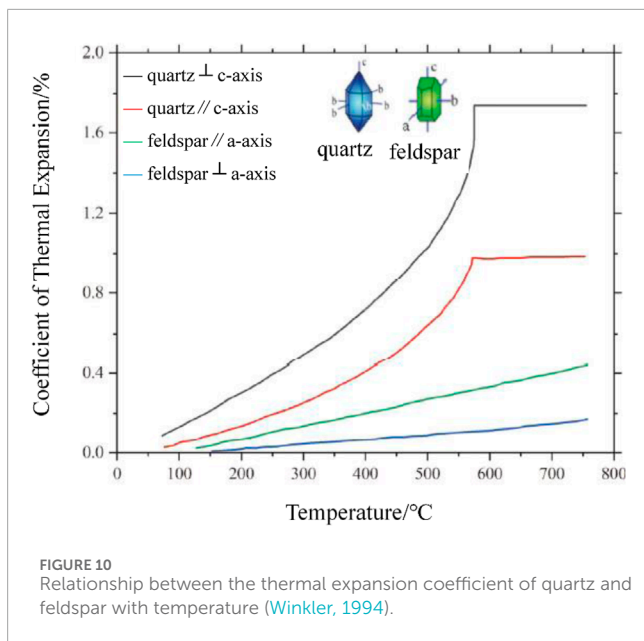
The elastic modulus can characterize the ability of the specimen to resist deformation, and the variation of elastic modulus can

TABLE 1 Failure modes of the layered sandstone specimens after heating and cooling treatments.

$T/^{\circ}\text{C}$ $\alpha/^{\circ}$	25	300	450	600	750
0					
30					
45					
60					
90					

better grasp the deformation characteristics of layered sandstone. Figure 8A depicts the elastic modulus of layered sandstone changes with  $\alpha$ , it can be seen that the elastic modulus of the specimens

is higher at different temperatures for  $\alpha = 0^{\circ}$  and  $90^{\circ}$ , while the minimum value of the elastic modulus occurs between  $30^{\circ}$  and  $60^{\circ}$ . The higher degree of specimen fragmentation at the temperature



of 750°C results in the elastic modulus of specimens with different laminar inclination angles at this temperature being lower than that at other temperatures. In Figure 8B, the correlation between the temperature and elastic modulus of sandstone is illustrated for every bedding angles. The figure illustrates that the rock experiences thermal cracks as a result of high temperature, which diminishes its resistance to deformation. Consequently, the elastic modulus gradually declines as the temperature rises from 25°C to 300°C. While the elastic modulus gradually increases as temperature rises from 300°C to 450°C. As the temperature rises from 450°C to 750°C, the elastic modulus of the specimen gradually decreases due to a phase transition occurring at approximately 573°C. This decrease is associated with alterations in the internal composition of the specimen.

Figure 9A illustrates the change in peak strain with  $\alpha$ , which is the axial strain at the point of maximum strength. According to the results, under the action of a certain temperature, the peak strain of the specimen reduced first, then increased, with increasing bedding

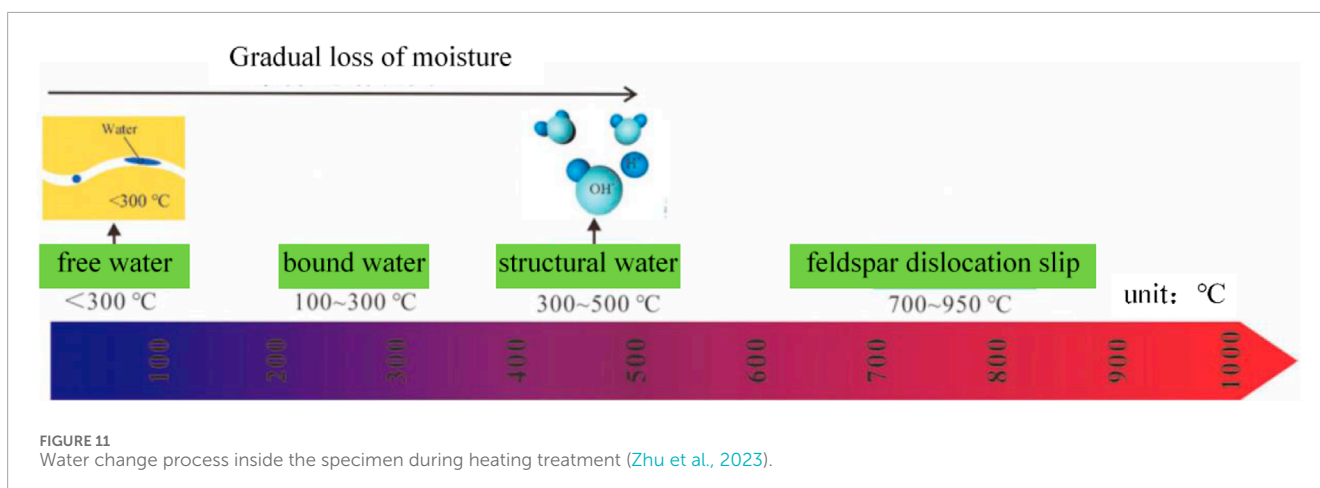
angle, and the peak strain was lowest at 60°. This is mainly due to the fact that the structure between the laminate is a weak zone, and the specimen is highly susceptible to damage when  $\alpha = 60^\circ$ , and the load carrying capacity reaches its limit at relatively small deformations.

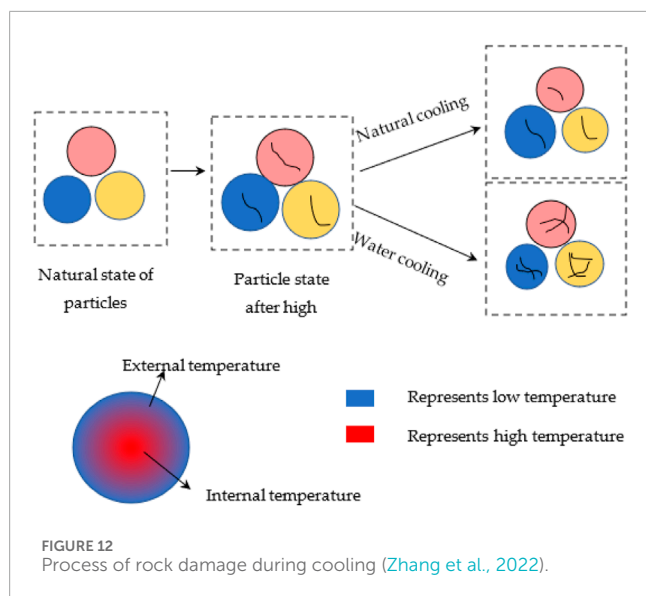
In Figure 9B, the correlation between peak strain and temperature is displayed, indicating that regardless of the bedding angle, the peak strain of the specimen rises as the temperature increases, and the rate of increase becomes progressively faster. That is, the variation is relatively gentle between 25°C and 300°C, while it is intensified at 600°C–750°C. In the case of  $\alpha = 30^\circ$ , the peak strain corresponding to 750°C is increased by 204% compared with that at 25°C. The rise in plastic deformation of the rock following heating and water-cooling treatment leads to an enhancement in the specimen’s ductile characteristics upon loading.

### 3.5 Failure mode

The failure modes of the layered sandstone specimens after undergoing heating and cooling treatments are displayed in Table 1. As the temperature and inclination angle vary, the failure modes undergo corresponding alterations. At  $\alpha = 0^\circ$ , the loading direction is orthogonal to the surface of the layer, and in this scenario, the layer has minimal impact on the damage mode, exhibiting damage in the form of axial splitting. When  $\alpha = 30^\circ$  or  $45^\circ$ , the effect of the weak layer structure on the specimen is more obvious, and the final damage mode is a mixed mode of axial split and slip along the layer. When  $\alpha = 60^\circ$ , the weak layer structure plays a decisive role in the damage mode of sandstone, which is the slip damage along the layer. At an angle of  $90^\circ$ , the layer aligns with the loading direction, resulting in lateral deformation caused by the Poisson effect when subjected to vertical load. Consequently, the damage pattern is characterized by tensile damage along the layer.

As the bedding angle reaches a specific point, the specimen’s damage escalates as the temperature rises. This is evident through the growing occurrence of cracks and spalling on the specimen’s surface. Nevertheless, once the temperature surpasses 750°C, the elevated heat degrades the sandstone structure, diminishing the impact of bedding tilt on the pattern





of deterioration, resulting primarily in cracks forming along the axial direction. After reaching a temperature of 750°C, the specimens' damage mode is primarily influenced by the temperature.

## 4 Discussion

### 4.1 Influence of bedding on the mechanical properties of rocks

Through the analysis of uniaxial mechanical properties of rocks with different angles of bed, it can be found that when  $\alpha = 60^\circ$ , the specimen is the most likely to be damaged, and the peak strength is also the lowest, which is due to the existence of the stratum that make the weak zone at the internal granular cementation of the rock, and the specimen is more prone to be damaged. Therefore, in the actual project, attention should be paid to the excavation direction, and try to avoid the 60° inclination area, so as to ensure the safety of the actual project.

### 4.2 Temperature effects on rocks

By observing and analyzing the microstructure of rocks following heating and water-cooling treatment, it becomes evident that changes in the mechanical characteristics of rocks are connected to the development of internal micro-cracks. The rock undergoes a series of micro-cracks due to the uneven expansion of its internal grains caused by temperature fluctuations, resulting in alterations to its mechanical characteristics. Furthermore, the varying expansion coefficients (parallel or perpendicular to a certain direction) of the particles within the rock when exposed to elevated temperatures result in a range of alterations in the rock, as depicted in Figure 10, and sandstone have high expansion values because of the presence of quartz. At a temperature of 100°C, water present in natural

rock will be released, whereas structural and tectonic water will be released at temperatures ranging from 100°C to 300°C and 300°C–500°C, respectively. Additionally, the water in the rock is free. At a temperature of 573°C, the quartz crystals within the rock experience a phase transition. As the temperature continues to rise, the internal metal bond of the specimen breaks, resulting in alterations to the rock's internal structure, as depicted in Figure 11.

The process of quickly cooling hot rock in a water bath is intricate, involving the rapid cooling of the initial high-temperature sample. The crack patterns become more intricate due to the temperature difference, as depicted in Figure 12. In practical engineering, the injection of cold water into hot rocks can result in increased damage and the formation of cracks, thereby causing issues in the actual project. Therefore, it is crucial to be mindful of these concerns in the relevant engineering tasks. Further, more cracks appeared in the rock under water cooling, and there was a certain variation in its strength along with the change in the composition of the particles during the heating treatment.

Conversely, the application of heat causes the depletion of both unbound and bound water in the rock, while also enhancing the cohesion of the clay minerals among the particles (Wu et al., 2019). Consequently, the temperature rise contributes to the augmentation of the durability of the sedimentary sandstone. In this study, it is necessary to take into account not just the impact of elevated temperatures but also the influence of water cooling. When the heating temperature is relatively low, the high temperature can only evaporate the free water and bound water, while the water cooling process, the grains and the clay minerals between them may reabsorb the water, resulting in a small change in strength, e.g., at  $T = 300^\circ\text{C}$ . Furthermore, when the temperature of the heating reaches 450°C, the water within the structure will vaporize. This water loss cannot be compensated for promptly during the cooling phase, leading to a rise in strength. As the temperature rises to 600°C, the moisture in the grains and clay minerals undergoes evaporation, resulting in a subsequent enhancement of the overall strength. Nevertheless, the strength enhancement is somewhat restricted due to the thermal fissures caused by the elevated temperature at this particular moment, as depicted in Figure 7, the rate of increase in uniaxial compressive strength has slowed down. As the temperature rises to 750°C, the load-bearing structure of the specimen experiences greater damage due to thermal cracks. The strength of the specimen is then governed by the cracking caused by thermal damage, resulting in a reduction in its overall strength. Currently, the specimen's failure mode is minimally influenced by the layer angle, but primarily governed by the thermal cracks, as indicated in Table 1.

The findings of this research can serve as a guide for the implementation of the real water-cooled rock initiative. Nevertheless, the impact of confining pressure was not considered in this study, and further investigations will be conducted on the scenario of rock confinement.

## 5 Conclusion

This study conducted uniaxial compressive tests on sandstone with varying laminar inclination after thermal treatment and rapid cooling in water. A comparative analysis was conducted on the

impact of dip angle and temperature on the mechanical properties and failure modes of sandstone. Additionally, the microscopic equipment was used to examine the fine structure of sandstone samples following water cooling after varying temperatures. These results unveiled the mechanical damage mechanism of layered sandstone subsequent to exposure to high temperatures and water cooling. Main conclusions can be summarized as follows:

- (1) The microscopic experimental results reveal that as the temperature rises, the presence, enlargement, and intersection of tiny cracks within the sample become increasingly apparent. This phenomenon is associated with the expansion of distinct particles within the sample and the occurrence of physicochemical reactions. The temperature within the sample rapidly decreases under cooling impact of water, intensifying the development of internal cracks due to the temperature difference.
- (2) The stress-strain of layered sandstone samples at various temperatures can be categorized into four phases: fracture compaction, elastic deformation, inelastic deformation, and destruction. As the inclination angle increases, the compaction phase of the specimen becomes more noticeable, resulting in a flatter curve at the early stages of loading.
- (3) The peak strength of the sample initially decreases and then increases as the dip angle increases, whereas with the rise in temperature, the peak strength follows a pattern of initial increase and subsequent decrease. The temperature has less impact on the elastic modulus, but it fluctuates as the temperature increases. The peak axial strain gradually rises as the temperature increases, but it decreases and then rises again as the inclination angle increases. The specimen's failure mode is affected by a mix of temperature and dip angle.

## Data availability statement

The original contributions presented in the study are included in the article/Supplementary material, further inquiries can be directed to the corresponding authors.

## References

- Cai, C. Z., Ren, K. D., Tao, Z. X., Xing, Y., Gao, F., Zou, Z. X., et al. (2022). Experimental investigation of the damage characteristics of high-temperature granite subjected to liquid nitrogen treatment. *Nat. Resour. Res.* 31, 2603–2627. doi:10.1007/s11053-022-10091-2
- Chen, Q. L., Yang, W. W., and Lu, H. (2022). Assessment of mechanical properties for high-temperature sandstone in coal fire area based on different cooling methods. *J. Civ. Eng.* 26 (12), 5187–5198. doi:10.1007/s12205-022-2112-z
- Ding, Q. L., Ju, F., Mao, X. B., Ma, D., Yu, B. Y., and Song, S. B. (2016). Experimental investigation of the mechanical behavior in unloading conditions of sandstone after high-temperature treatment. *Rock Mech. Rock Eng.* 49 (7), 2641–2653. doi:10.1007/s00603-016-0944-x
- Donath, F. A. (1972). Effects of cohesion and granularity on deformational behaviour anisotropic rock, in studies in mineralogy and Precambrian geology. *Geol. Soc. Amer. Mem.* 135, 95–128.
- Dong, Z. H., Sun, Q., Ye, J., and Zhang, W. Q. (2020). Changes in color and roughness of red sandstone at high temperatures. *B. Eng. Geol. Environ.* 79, 1959–1966. doi:10.1007/s10064-019-01678-w
- Dunn, D. E., Lafountain, L. J., and Jackson, R. E. (1973). Porosity dependence and mechanism of brittle fracture in sandstones. *J. Geophys. Res.* 78, 2403–2417. doi:10.1029/jb078i014p02403
- Fan, L. F., Gao, J. W., Du, X. L., and Wu, Z. J. (2020). Spatial gradient distributions of thermal shock-induced damage to granite. *J. Rock Mech. Geotech. Eng.* 12 (5), 917–926. doi:10.1016/j.jrmge.2020.05.004
- Gautam, P. K., Verma, A. K., Jha, M. K., Sharma, P., and Singh, T. N. (2018). Effect of high temperature on physical and mechanical properties of Jalore granite. *J. Appl. Geophys.* 159, 460–474. doi:10.1016/j.jappgeo.2018.07.018
- Gautam, P. K., Verma, A. K., Maheshwar, S., and Singh, T. N. (2016). Thermomechanical analysis of different types of sandstone at elevated temperature. *Rock Mech. Rock Eng.* 49 (5), 1985–1993. doi:10.1007/s00603-015-0797-8
- Guo, X., Zou, G. F., Wang, Y. H., Wang, Y., and Gao, T. (2017). Investigation of the temperature effect on rock permeability sensitivity. *J. Pet. Sci. Eng.* 156, 616–622. doi:10.1016/j.petrol.2017.06.045
- Hu, S. C., Tan, Y. L., Hui, Z., Guo, W. Y., Hu, D. W., Meng, F. Z., et al. (2017). Impact of bedding planes on mechanical properties of sandstone. *Rock Mech. Rock Eng.* 50 (8), 2243–2251. doi:10.1007/s00603-017-1239-6

## Author contributions

JX: Conceptualization, Data curation, Formal Analysis, Methodology, Writing—original draft, Writing—review and editing. W-LT: Project administration, Writing—review and editing. Y-SB: Software, Writing—review and editing. JY: Software, Writing—review and editing.

## Funding

The author(s) declare that no financial support was received for the research, authorship, and/or publication of this article.

## Acknowledgments

The authors would like to extend their heartfelt appreciation to the editor and unidentified reviewers for their valuable feedback, which has significantly enhanced the quality of this manuscript.

## Conflict of interest

The authors declare that the research was conducted in the absence of any commercial or financial relationships that could be construed as a potential conflict of interest.

## Publisher's note

All claims expressed in this article are solely those of the authors and do not necessarily represent those of their affiliated organizations, or those of the publisher, the editors and the reviewers. Any product that may be evaluated in this article, or claim that may be made by its manufacturer, is not guaranteed or endorsed by the publisher.

- Huang, Y. H., Yang, S. Q., Tian, W. L., Zhao, J., Ma, D., and Zhang, C. S. (2017). Physical and mechanical behavior of granite containing pre-existing holes after high temperature treatment. *Arch. Civ. Mech. Eng.* 17 (4), 912–925. doi:10.1016/j.acme.2017.03.007
- Kang, F. C., Jia, T. R., Li, Y. C., Deng, J. H., Tang, C. A., and Huang, X. (2021). Experimental study on the physical and mechanical variations of hot granite under different cooling treatments. *Renew. Energy* 179, 1316–1328. doi:10.1016/j.renene.2021.07.132
- Liu, S., and Xu, J. Y. (2014). Mechanical properties of Qinling biotite granite after high temperature treatment. *Int. J. Rock Mech. Min. Sci.* 71, 188–193. doi:10.1016/j.ijrmms.2014.07.008
- Ma, D., Duan, H. Y., and Zhang, J. X. (2022c). Solid grain migration on hydraulic properties of fault rocks in underground mining tunnel: Ra-dial seepage experiments and verification of permeability prediction. *Tunn. Undergr. Space Technol.* 126, 104525. doi:10.1016/j.tust.2022.104525
- Ma, D., Duan, H. Y., Zhang, J. X., and Bai, H. B. (2022b). A state-of-the-art review on rock seepage mechanism of water inrush disaster in coal mines. *Int. J. Coal Sci. Technol.* 9, 50. doi:10.1007/s40789-022-00525-w
- Ma, D., Duan, H. Y., Zhang, J. X., Liu, X. W., and Li, Z. H. (2022a). Numerical simulation of water-silt inrush hazard of fault rock: a three-phase flow model. *Rock Mech. Rock Eng.* 55, 5163–5182. doi:10.1007/s00603-022-02878-9
- Nin, P., Ju, F., Su, H. J., He, Z. Q., Xiao, M., Zhang, Y. Z., et al. (2021). An investigation on the deterioration of physical and mechanical properties of granite after cyclic thermal shock. *Geothermics* 97, 102252. doi:10.1016/j.geothermics.2021.102252
- Ranjith, P. G., Viete, D. R., Chen, B. J., and Perera, M. S. A. (2012). Transformation plasticity and the effect of temperature on the mechanical behaviour of Hawkesbury sandstone at atmospheric pressure. *Eng. Geol.* 151, 120–127. doi:10.1016/j.enggeo.2012.09.007
- Rawling, G. C., Baud, P., and Wong, T. F. (2002). Dilatancy, brittle strength, and anisotropy of foliated rocks: experimental deformation and micromechanical modeling. *J. Geophys. Res.* 107 (B10), 1–14. doi:10.1029/2001jb000472
- Shi, X. S., Jing, H. W., Yin, Q., Zhao, Z. L., Han, G. S., and Gao, Y. (2020). Investigation on physical and mechanical properties of bedded sandstone after high-temperature exposure. *B. Eng. Geol. Environ.* 79, 2591–2606. doi:10.1007/s10064-020-01729-7
- Sirdesai, N. N., Singh, T. N., and Pathgama, G. R. (2017b). Thermal alterations in the poro-mechanical characteristic of an Indian sandstone: a comparative study. *Eng. Geol.* 226, 208–220. doi:10.1016/j.enggeo.2017.06.010
- Sirdesai, N. N., Singh, T. N., Ranjith, P. G., and Singh, R. (2017a). Effect of varied durations of thermal treatment on the tensile strength of red sandstone. *Rock Mech. Rock Eng.* 50 (1), 205–213. doi:10.1007/s00603-016-1047-4
- Su, H. J., Jing, H. W., Du, M. R., and Wang, C. (2016). Experimental investigation on tensile strength and its loading rate effect of sandstone after high temperature treatment. *Arab. J. Geosci.* 9 (13), 616. doi:10.1007/s12517-016-2639-8
- Sun, Q., Zhang, W. Q., Su, T. M., and Zhu, S. Y. (2016). Variation of wave velocity and porosity of sandstone after high temperature heating. *Acta Geophys.* 64 (3), 633–648. doi:10.1515/ageo-2016-0021
- Wasantha, P. L. P., Ranjith, P. G., and Shao, S. S. (2014). Energy monitoring and analysis during deformation of bedded-sandstone: use of acoustic emission. *Ultrasonics* 54, 217–226. doi:10.1016/j.ultras.2013.06.015
- Winkler, E. M. (1994). *Stone in architecture: properties, durability*[C]. Berlin, Germany: Springer.
- Wu, X. G., Huang, Z. W., Song, H. Y., Zhang, S. K., Cheng, Z., Li, R., et al. (2019). Variations of physical and mechanical properties of heated granite after rapid cooling with liquid nitrogen. *Rock Mech. Rock Eng.* 52, 2123–2139. doi:10.1007/s00603-018-1727-3
- Wu, X. H., Guo, Q., Zhu, Y., Ren, F., Zhang, J., Wu, X., et al. (2021). Pore structure and crack characteristics in high-temperature granite under water-cooling. *Case Stud. Therm. Eng.* 28, 101646. doi:10.1016/j.csite.2021.101646
- Yan, B. Q., Kang, H. P., Zuo, J. P., Wang, P. T., Li, X. S., Cai, M. F., et al. (2023). Study on damage anisotropy and energy evolution mechanism of jointed rock mass based on energy dissipation theory. *B. Eng. Geol. Environ.* 82, 294. doi:10.1007/s10064-023-03278-1
- Yang, R. Y., Huang, Z. W., Shi, Y., Yang, Z. Q., and Huang, P. P. (2019). Laboratory investigation on cryogenic fracturing of hot dry rock under triaxial-confining stresses. *Geothermics* 79, 46–60. doi:10.1016/j.geothermics.2019.01.008
- Yang, S. Q., Dong, Z. J., Huang, Y. H., and Teng, S. Y. (2021). An experimental study on physical, mechanical and CO<sub>2</sub> permeability behavior of sandstone after high temperature treatment. *J. Test. Eval.* 49 (3), 1433–1453. doi:10.1520/jte20190915
- Yang, S. Q., Li, Y., Ma, G. W., Sun, B. W., Yang, J., Xu, J., et al. (2023). Experiment and numerical simulation study of dynamic mechanical behavior of granite specimen after high temperature treatment. *Comput. Geotech.* 154, 105111. doi:10.1016/j.compgeo.2022.105111
- Yang, S. Q., Ranjith, P. G., Jing, H. W., Tian, W. L., and Ju, Y. (2017). An experimental investigation on thermal damage and failure mechanical behavior of granite after exposure to different high temperature treatments. *Geothermics* 65, 180–197. doi:10.1016/j.geothermics.2016.09.008
- Yang, Z. Y., Chen, J. M., and Huang, T. H. (1998). Effect of joint sets on the strength and deformation of rock mass models. *Int. J. Rock Mech. Min. Sci.* 35 (1), 75–84. doi:10.1016/s0148-9062(97)83478-x
- Yin, P. F., and Yang, S. Q. (2018). Experimental investigation of the strength and failure behavior of layered sandstone under uniaxial compression and Brazilian testing. *Acta geophys.* 66 (4), 585–605. doi:10.1007/s11600-018-0152-z
- Zhang, J. S., Lu, Y., Pang, J. Y., and Bu, Y. S. (2022). Experimental study on mechanical properties of high temperature granite with different cooling methods. *Appl. Sci.* 12 (12), 5968. doi:10.3390/app12125968
- Zhang, M. L., Qiu, R. D., Yang, L., and Su, Y. T. (2020). Experimental research on mechanical properties of high-temperature sandstone with different cooling methods. *Adv. Civ. Eng.*, 8879760.
- Zhang, W. Q., Sun, Q., Hao, S. Q., Geng, J. S., and Lv, C. (2016). Experimental study on the variation of physical and mechanical properties of rock after high temperature treatment. *Appl. Therm. Eng.* 98, 1297–1304. doi:10.1016/j.applthermaleng.2016.01.010
- Zhang, W. Q., Sun, Q., Zhu, Y. M., and Guo, W. H. (2019). Experimental study on response characteristics of micro-macroscopic performance of red sandstone after high-temperature treatment. *J. Therm. Anal. Calorim.* 136, 1935–1945. doi:10.1007/s10973-018-7880-9
- Zhang, X. M., Yang, J. S., and Liu, B. C. (2010). Experimental study on anisotropic strength properties of sandstone. *Electron. J. Geotech. Eng.* 15, 1325–1335.
- Zhao, X. G., Zhao, Z., Guo, Z., Cai, M., Li, X., Li, P. F., et al. (2018). Influence of thermal treatment on the thermal conductivity of Beishan granite. *Rock Mech. Rock Eng.* 51, 2055–2074. doi:10.1007/s00603-018-1479-0
- Zhao, Y. C., Huang, M., Jiang, Y. J., and Wang, Z. (2023). Mechanics, damage and energy degradation of rock-concrete interfaces exposed to high temperature during cyclic shear. *Constr. Build. Mat.* 105, 133229.
- Zhou, X. P., Li, G. Q., and Ma, H. C. (2020). Real-time experiment investigations on the coupled thermomechanical and cracking behaviors in granite containing three pre-existing fissures. *Eng. Fract. Mech.* 224, 106797. doi:10.1016/j.engfractmech.2019.106797
- Zhou, Z. L., Cai, X., Ma, D., Du, X., Chen, L., Wang, H., et al. (2019). Water saturation effects on dynamic fracture behavior of sandstone. *Int. J. Rock Mech. Min. Sci.* 114, 46–61. doi:10.1016/j.ijrmms.2018.12.014
- Zhu, Z. N., Kempka, T., Rangith, P. G., Tian, H., Jiang, G., Dou, B., et al. (2021). Changes in thermomechanical properties due to air and water cooling of hot dry granite rocks under unconfined compression. *Renew. Energy* 170, 562–573. doi:10.1016/j.renene.2021.02.019
- Zhu, Z. N., Tian, H., Jiang, G. S., and Cheng, W. (2018). Effects of high temperature on the mechanical properties of Chinese marble. *Rock Mech. Rock Eng.* 51 (6), 1937–1942. doi:10.1007/s00603-018-1426-0
- Zhu, Z. N., Wang, D. Y., Yang, S. Q., Jie, J. Y., Yuan, Y. L., Wu, T. Y., et al. (2023). Comparative study of permeability evolution characteristics of dry hot granite under different cooling rates. *J. Rock Mech. Eng.*, 1–14. [in Chinese].